A Rare Example of Three Abundant Conformers in One Retro Model of the Cisplatin−DNA d(GpG) Intrastrand Cross Link. Unambiguous Evidence That Guanine O6 to Carrier Amine Ligand Hydrogen Bonding Is Not Important. Possible Effect of the Lippard Base Pair Step Adjacent to the Lesion on Carrier Ligand Hydrogen Bonding in DNA Adducts

Sharon T. Sullivan,[‡] Antonella Ciccarese,[†] Francesco P. Fanizzi,[†,§] and Luigi G. Marzilli*[,‡]

Dipartimento di Biologia, Università di Lecce, Via Monteroni, I-73100 Lecce, Italy, Cancer Research Center, Consortium C.A.R.S.O., I-70010 Valenzano-Bari, Italy, and Department of Chemistry, Emory University, Atlanta, Georgia 30322

Received February 22, 2001. Revised Manuscript Received June 22, 2001

Abstract: Guanine O6 to carrier ligand hydrogen bonding is a central feature of many hypotheses advanced to explain the anticancer activity of cis-type anticancer drugs, *cis*-PtA_2X_2 (A_2 = diamine or two amines). Early structural evidence suggested that *cis*-$Pt(NH_3)_2$(d(GpG)) (the cross-link model for the key cisplatin−DNA adduct) and other *cis*-PtA_2(d(GpG)) adducts exist exclusively or mainly as the HH1 conformer with head-to-head (HH) bases. The dynamic motion of the d(GpG) in these adducts is too rapid to permit definitive characterization of both the conformation and the H-bonding. Hence, we use retro models having A_2 ligands designed to slow the motion. Here, we employ **Me$_2$ppz** (*N*,*N*′-dimethylpiperazine), which lacks NH groups. **Me$_2$ppz** is unique in having sp^3 *N*-methyl groups directly in the coordination plane, allowing the coexistence of multiple conformers but hindering dynamic motion in **Me$_2$ppz**Pt(d(GpG)) and **Me$_2$ppz**Pt(GpG) retro models. Dynamic processes are decreased enough in **Me$_2$ppz**Pt(d(GpG)) to permit HPLC separation of three abundant forms. After HPLC separation, the three re-equilibrate, proving that the three forms must be conformers and that **Me$_2$ppz** has little influence on conformer distribution. This marks the first reported characterization of *three* abundant conformers for *one cis*-PtA_2(d(GpG)) adduct. From NMR evidence, the **Me$_2$ppz**Pt(d(GpG)) HH1 conformer has uncanted bases. Another conformer, one of two recently discovered conformer types, has head-to-tail (HT) bases with Δ chirality. For this ΔHT1 form, several lines of evidence establish that the dinucleotide moieties have essentially identical structures in d(GpG) (and GpG) adducts of **Me$_2$ppz**Pt and other *cis*-PtA_2 complexes. For example, the shifts of the highly structure-sensitive G H8 NMR signals are almost identical for the ΔHT1 form of all adducts. In previous models, the stabilization of the ΔHT1 form could be attributed to G O6 H-bonding to A_2 NH groups. Such H-bonds are not possible for **Me$_2$ppz**. The unambiguous conclusions are that G O6 H-bonding is weak and that neither canting nor H-bonding is essential in HH forms. These two features are present in almost all other small models but are essentially absent in the cross-link base pair (bp) step in duplexes. We conclude from our work that the forces favoring canting and H-bonding are weak, and we hypothesize that steric effects within the Lippard bp step adjacent to this cross-link bp step easily overcome these forces.

Introduction

Pt Anticancer Activity and Carrier Ligand NH Groups. A higher percentage of platinum compounds exhibit anticancer activity compared to compounds of all other types.[1−4] The vast majority of Pt anticancer compounds have NH-bearing carrier ligands retained after the drug binds its DNA target.[1,2,5−7] Such observations have led to a number of hypotheses about hydrogen-bonding interactions of the NH group with the target, both during and after DNA adduct formation.[1,5,7−16] The anticancer activity of cisplatin (*cis*-$Pt(NH_3)_2Cl_2$), an important

* To whom correspondence should be addressed. E-mail: lmarzil@emory.edu.
† Università di Lecce.
‡ Emory University.
§ Consortium C.A.R.S.O.

(1) Bloemink, M. J.; Reedijk, J. In *Metal Ions in Biological Systems*; Sigel, A., Sigel, H., Eds.; Marcel Dekker: New York, 1996; Vol. 32, pp 641−685.
(2) *Cisplatin: Chemistry and Biochemistry of a Leading Anticancer Drug*; Lippert, B., Ed.; Wiley-VCH: Weinheim, 1999; pp 1−556.
(3) Abrams, M. J. In *The Chemistry of Antitumour Agents*; Wilman, D. E. V., Ed.; Chapman and Hall: New York, 1990; pp 331−341.
(4) Keppler, B. K.; Vogel, E. A. In *Platinum and Other Metal Coordination Compounds in Cancer Chemotherapy 2*; Pinedo, H. M., Schornagel, J. H., Eds.; Plenum Press: New York, 1996; pp 253−268.
(5) Reedijk, J. *Chem. Commun.* **1996**, 801−806.
(6) Sherman, S. E.; Lippard, S. J. *Chem. Rev.* **1987**, *87*, 1153−1181.
(7) Jamieson, E. R.; Lippard, S. J. *Chem. Rev.* **1999**, *99*, 2467−2498.
(8) van Garderen, C. J.; Bloemink, M. J.; Richardson, E.; Reedijk, J. *J. Inorg. Biochem.* **1991**, *42*, 199−205.
(9) Reedijk, J. *Inorg. Chim. Acta* **1992**, *198*−*200*, 873−881.
(10) Bloemink, M. J.; Lempers, E. L. M.; Reedijk, J. *Inorg. Chim. Acta* **1990**, *176*, 317−320.
(11) Sherman, S. E.; Gibson, D.; Wang, A.; Lippard, S. J. *J. Am. Chem. Soc.* **1988**, *110*, 7368−7381.

10.1021/ja010483m CCC: $20.00
Published on Web 08/31/2001

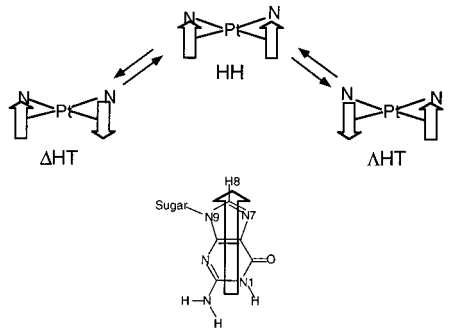

Figure 1. Schematic representation of possible base orientations of two cis G bases coordinated to Pt. G coordination sites are forward, platinum carrier ligand is to the rear. Arrows represent G bases (shown below scheme). Interconversion between these conformers is possible via rotation about the Pt−G N7 bond.

member of the most widely used *cis*-PtA_2X_2 drug type (A_2 = two amines or a diamine), is widely attributed to the formation of an adduct involving two adjacent guanines of d(GpG) sequences in DNA, cross-linked to Pt at the N7 atoms.[1,5,6] Thus, evaluating hydrogen-bonding interactions with the G residue is important and requires a good knowledge of adduct structure. Since structures of adducts of polymeric nucleic acids are normally imprecise, three classes of synthetic models have been utilized. The most faithful are DNA oligonucleotide duplexes with intrastrand and interstrand G*−Pt−G* cross-links. (G* = G platinated at N7 in DNA or oligonucleotides longer than a dinucleotide.) Next, adducts with single strands have been studied as models of the intrastrand cross-link. Finally, simplest of all are complexes with Pt−**G** moieties (bold **G** = unlinked guanine derivative).

We focus here on cisplatin. The *cis*-$Pt(NH_3)_2$(d(GpG)) N7−Pt−N7 intrastrand cross-link lesion has been widely accepted to adopt primarily a head-to-head (HH) arrangement (Figure 1), with both G's maintaining the B-DNA anti conformation,[1,6,11,17−21] which we call HH1. In contrast, the G bases adopt a head-to-tail (HT) arrangement with Δ chirality (Figure 1) in interstrand adducts,[22−25] which could also contribute to the anticancer activity.[26,27]

Examination of an X-ray structure of an HMG-bound 16-oligomer[28] and an X-ray/NMR-derived model of a duplex 9-oligomer[29] (both containing the intrastrand cisplatin lesion) suggests that such hydrogen-bonding interactions involving the NH_3 ligands are weak and may not exist. Furthermore, if the ammonia groups are replaced by A_2 carrier ligands having sp^3 N's bearing two or more alkyl groups, the 9-mer structure suggests that clashes will result.[29] Carrier ligand−DNA H-bonds are also absent in the crystal structure of a cisplatin interstrand adduct.[25] These findings on duplex models have led us to a new hypothesis: "The very small size of the NH group, not its hydrogen-bonding ability, is responsible for the good activity exhibited by Pt compounds with amine carrier ligands bearing multiple NH groups."

This hypothesis must be tested further for several reasons. First, the size of duplex models limits the accuracy of the structures. Second, many examples of hydrogen bonding have been found in accurately determined solid-state structures of small models.[30−32] Third, results on duplexes in solution were recently interpreted to suggest that H-bonding occurred.[33] Fourth, long G O6 to carrier ligand N distances, indicating the absence of hydrogen bonding, are linked to an unusual feature, a base pair (bp) step in which the shift and slide both have a large positive value.[28] This "Lippard base pair step" is the step between the bp containing the 5′-G* and the bp adjacent to the 5′-G*. The G*G* and the Lippard bp steps contain the largest departures from the B-form structure. Both bp steps thus contain key structural features of the lesion. The mutual influence of the carrier ligand and its NH groups, of the cross-link bp step, and of the Lippard bp step must be evaluated in future research on Pt-induced DNA distortions. *As a necessary first step*, we report here a dinucleotide "retro model"[34,35] of the cross-link bp step with a carrier ligand lacking NH groups. The retro-model approach is discussed below after the background for the method is presented.

Background. The small size of the NH group permits a high dynamic character that decreases the utility of NMR data and obscures the relationship between solution and solid-state structures. *cis*-$PtA_2\mathbf{G}_2$ adducts with A_2 = ammonia or nonbulky NH-bearing carrier ligands exhibit only one set of **G** NMR resonances,[36,37] a result attributed to rapid rotation of both **G**'s about the Pt−**G** N7 bonds, allowing interconversion between HH and HT forms (Figure 1) that is fast on the NMR time scale.[24,36] These dynamic models can be assumed to be mainly the two HT forms with Δ and Λ chirality in almost equal abundance on the basis of both solution and solid-state data.[24,30,36,38−44]

(12) Farrell, N. In *Metal Ions in Biological Systems*; Sigel, A., Sigel, H., Eds.; Marcel Dekker: New York, 1996; Vol. 32, pp 603−639.
(13) Cleare, M. J.; Hoeschele, J. D. *Bioinorg. Chem.* **1973**, *2*, 187−210.
(14) Laoui, A.; Kozelka, J.; Chottard, J.-C. *Inorg. Chem.* **1988**, *27*, 2751−2753.
(15) Bloemink, M. J.; Heetebrij, R. J.; Inagaki, K.; Kidani, Y.; Reedijk, J. *Inorg. Chem.* **1992**, *31*, 4656−4661.
(16) Bloemink, M. J.; Dorenbos, J. P.; Heetebrij, R. J.; Keppler, B. K.; Reedijk, J.; Zahn, H. *Inorg. Chem.* **1994**, *33*, 1127−1132.
(17) Yang, D.; van Boom, S.; Reedijk, J.; van Boom, J.; Wang, A. *Biochemistry* **1995**, *34*, 12912−12920.
(18) den Hartog, J. H. J.; Altona, C.; Chottard, J.-C.; Girault, J.-P.; Lallemand, J.-Y.; de Leeuw, F. A.; Marcelis, A. T. M.; Reedijk, J. *Nucleic Acids Res.* **1982**, *10*, 4715−4730.
(19) Girault, J.-P.; Chottard, G.; Lallemand, J.-Y.; Chottard, J.-C. *Biochemistry* **1982**, *21*, 1352−1356.
(20) Chottard, J. C.; Girault, J.-P.; Chottard, G.; Lallemand, J.-Y.; Mansuy, D. *J. Am. Chem. Soc.* **1980**, *102*, 5565−5572.
(21) Kozelka, J.; Fouchet, M. H.; Chottard, J.-C. *Eur. J. Biochem.* **1992**, *205*, 895−906.
(22) Huang, H.; Zhu, L.; Drobny, G. P.; Hopkins, P. B.; Reid, B. R. *Science* **1995**, *270*, 1842−1845.
(23) Paquet, F.; Perez, C.; Leng, M.; Lancelot, G.; Malinge, J.-M. *J. Biomol. Struct. Dyn.* **1996**, *14*, 67−77.
(24) Ano, S. O.; Kuklenyik, Z.; Marzilli, L. G. In *Cisplatin. Chemistry and Biochemistry of a Leading Anticancer Drug*; Lippert, B., Ed.; Wiley-VCH: Weinheim, 1999; pp 247−291.
(25) Coste, F.; Malinge, J.-M.; Serre, L.; Shepard, W.; Roth, M.; Leng, M.; Zelwer, C. *Nucleic Acids Res.* **1999**, *27*, 1837−1846.
(26) Pinto, A. L.; Lippard, S. J. *Biochim. Biophys. Acta* **1985**, *780*, 167−180.
(27) van der Veer, J. L.; Reedijk, J. *Chem. Br.* **1988**, *24*, 775−780.
(28) Ohndorf, U.-M.; Rould, M. A.; He, Q.; Pabo, C. O.; Lippard, S. J. *Nature* **1999**, *399*, 708−712.
(29) Marzilli, L. G.; Saad, J. S.; Kuklenyik, Z.; Keating, K. A.; Xu, Y. *J. Am. Chem. Soc.* **2001**, *123*, 2764−2770.
(30) Lippert, B.; Raudaschl, G.; Lock, C. J. L.; Pilon, P. *Inorg. Chim. Acta* **1984**, *93*, 43−50.
(31) Schöllhorn, H.; Raudaschl-Sieber, G.; Müller, G.; Thewalt, U.; Lippert, B. *J. Am. Chem. Soc.* **1985**, *107*, 5932−5937.
(32) Sindellari, L.; Schöllhorn, H.; Thewalt, U.; Raudaschl-Sieber, G.; Lippert, B. *Inorg. Chim. Acta* **1990**, *168*, 27−32.
(33) Malina, J.; Hofr, C.; Maresca, L.; Natile, G.; Brabec, V. *Biophys. J.* **2000**, *78*, 2008−2021.
(34) Marzilli, L. G.; Ano, S. O.; Intini, F. P.; Natile, G. *J. Am. Chem. Soc.* **1999**, *121*, 9133−9142.
(35) Williams, K. M.; Cerasino, L.; Natile, G.; Marzilli, L. G. *J. Am. Chem. Soc.* **2000**, *122*, 8021−8030.
(36) Cramer, R. E.; Dahlstrom, P. L. *J. Am. Chem. Soc.* **1979**, *101*, 3679−3681.
(37) Dijt, F. J.; Canters, G. W.; den Hartog, J. H.; Marcelis, A. T. M.; Reedijk, J. *J. Am. Chem. Soc.* **1984**, *106*, 3644−3647.

Despite efforts by workers in many laboratories, *cis*-Pt$(NH_3)_2$(d(GpG)), the simplest cross-link model, has never been characterized by X-ray methods. The fact that this model has only one set of ^{1}H NMR signals[18,19] has been taken to imply that this cross-link model favors the HH1 conformer, which undergoes slow Pt−G N7 bond rotation.[1,18,19,21,45,46] The phosphate backbone of the dinucleotide is thought to stabilize an HH arrangement, thereby rendering an HT form less favorable in *cis*-PtA_2(d(GpG)) cross-linked models.[11,47] Thus, the observation of only one set of ^{1}H NMR resonances for both the *cis*-PtA_2**G**$_2$ and the *cis*-PtA_2(d(GpG)) models had two contrasting interpretations, a difficulty we named the "dynamic motion problem".[24,47]

The fluxional properties of models with ammonia or carrier ligands with NH_2 donors cause other problems. The position of the NH groups can fluctuate. Guanine coordination via N7 to Pt places the G O6 within reach of an NH of the cis amine. Thus, hydrogen bonding in water is difficult to assess. The solid state could favor a hydrogen bond or even a conformer[44] that either may not be present or may be of minor importance in water. As a result, there are many examples of G O6−NH hydrogen bonds in the solid state.[30−32,48,49]

Retro Models. To overcome these problems, we use the "retro-modeling" approach with carrier ligands designed to have features that simultaneously make the spectral properties more informative, reduce the dynamic motion by about a billion-fold compared to *cis*-Pt$(NH_3)_2$ adducts, and permit the coexistence of multiple conformers, as is possible in adducts with amine donors found in anticancer drugs.[24,42,43] Our most successful carrier ligand, 2,2′-bipiperidine (**Bip**),[24,35,42,47,50] has two favorable coordinated **Bip** configurations (*S*,*R*,*R*,*S* or *R*,*S*,*S*,*R* configurations at the asymmetric N, C, C, and N chelate ring atoms) (Figure 2). *Note that we denote diamine carrier ligands in boldface type.* Because each amine donor carries only one nondynamic NH group, such retro models reduce the problems in assessing hydrogen bonding; furthermore, the nearby chiral carbon both defines the secondary amine chirality and restricts the NH group position in space.[24,42,43,51−53]

The **Bip** configuration controls which chirality (Δ or Λ, Figure 1) of the **Bip**Pt**G**$_2$ HT conformers is preferred.[42,43,50] The

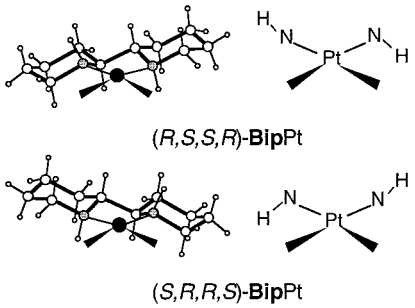

Figure 2. Both ball-and-stick and shorthand notation for **Bip**Pt, with stereochemistry for N, C, C, and N chelate ring atoms.

Chart 1. Schematic Drawing Showing the Favored ΛHT Conformer for (*S*,*R*,*R*,*S*)-**Bip**PtG_2 Complexes (Upper Left) and the ΔHT1 Conformer for the (*S*,*R*,*R*,*S*)-**Bip**Pt(d(GpG)) Adduct (Upper Right)[a]

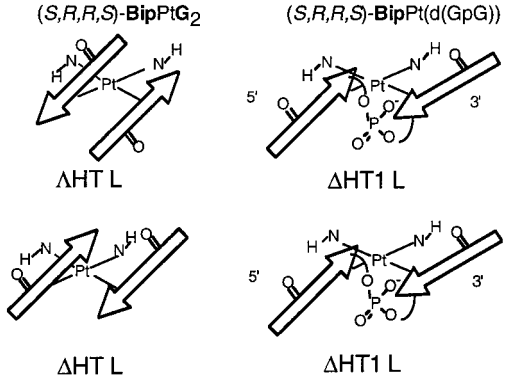

[a] This **Bip** configuration favors left-handed canting. In the unlinked model, **G** base canting minimizes carrier ligand−**G** O6 steric clashes, and the base orientation allows water to access the NH group. In the linked model, the G O6 is closer to the NH group, opening the possibility that G O6 to NH H-bonding stabilizes the structure. On N1H deprotonation, the HT chirality changes for the unlinked model (lower left) but not for the linked model (lower right).

favored conformer has **G** O6 on the wrong and the correct side of the coordination plane for hydrogen bonding for **G** and N1 deprotonated **G** (**G**$^-$), respectively (Chart 1).[42,43] These results indicate the following order of NH hydrogen-bonding strength *in water*: **G**$^-$ O6 > water > **G** O6.[42,43,51,52] This interpretation that guanine O6 > carrier ligand hydrogen-bond interactions are inherently weak is consistent with other work[54] and with our hypothesis that the small size of the hydrogen atom is the important feature of NH-bearing carrier ligands. However, the conformer preferred is influenced by "second-sphere communication", i.e., the interaction of the phosphate group of one guanine derivative with the base of the cis guanine derivative.[43,51−53] These complications and the results to be summarized next on **Bip**Pt(d(GpG)) adducts indicate clearly the need for additional tests of the "small size" hypothesis.

(*S*,*R*,*R*,*S*)-**Bip**Pt(d(GpG))[34] and (*R*,*S*,*S*,*R*)-**Bip**Pt(d(GpG)),[47] isomers with the enantiomeric configuration of the **Bip** ligand, each have *two* major conformers with similar populations. Each has the well-known HH1 form, but the canting direction differs in each. (*S*,*R*,*R*,*S*)-**Bip**Pt(d(GpG)) has left-handed canted conformers, HH1 L and *anti*,*syn*-ΔHT1 L (HT bases with the Δ chirality and normal phosphodiester backbone propagation direction, *anti*-5′- and *syn*-3′-G) (Figure 3). (*R*,*S*,*S*,*R*)-**Bip**Pt(d(GpG)) has right-handed conformers, HH1 R and HH2 R (a new conformer differing from HH1 in the direction of propaga-

(38) Cramer, R. E.; Dahlstrom, P. L. *Inorg. Chem.* **1985**, *24*, 3420−3424.
(39) Isab, A. A.; Marzilli, L. G. *Inorg. Chem.* **1998**, *37*, 6558−6559.
(40) Cramer, R. E.; Dahlstrom, P. L.; Seu, M. J. T.; Norton, T.; Kashiwagi, M. *Inorg. Chem.* **1980**, *19*, 148−154.
(41) Orbell, J. D.; Taylor, M. R.; Birch, S. L.; Lawton, S. E.; Vilkins, L. M. *Inorg. Chim. Acta* **1988**, *152*, 125−134.
(42) Ano, S. O.; Intini, F. P.; Natile, G.; Marzilli, L. G. *Inorg. Chem.* **1999**, *38*, 2989−2999.
(43) Marzilli, L. G.; Intini, F. P.; Kiser, D.; Wong, H. C.; Ano, S. O.; Marzilli, P. A.; Natile, G. *Inorg. Chem.* **1998**, *37*, 6898−6905.
(44) Wong, H. C.; Shinozuka, K.; Marzilli, L. G. *Inorg. Chim. Acta* **2000**, *297*, 36−46.
(45) Neumann, J.-M.; Tran-Dinh, S.; Girault, J.-P.; Chottard, J.-C.; Huynh-Dinh, T.; Igolen, J. *Eur. J. Biochem.* **1984**, *141*, 465−472.
(46) Berners-Price, S. J.; Ranford, J. D.; Sadler, P. J. *Inorg. Chem.* **1994**, *33*, 5842−5846.
(47) Ano, S. O.; Intini, F. P.; Natile, G.; Marzilli, L. G. *J. Am. Chem. Soc.* **1998**, *120*, 12017−12022.
(48) Grabner, S.; Plavec, J.; Bukovec, N.; Di Leo, D.; Cini, R.; Natile, G. *J. Chem. Soc., Dalton Trans.* **1998**, 1447−1451.
(49) Cini, R.; Grabner, S.; Bukovec, N.; Cerasino, L.; Natile, G. *Eur. J. Inorg. Chem.* **2000**, 1601−1607.
(50) Ano, S. O.; Intini, F. P.; Natile, G.; Marzilli, L. G. *J. Am. Chem. Soc.* **1997**, *119*, 8570−8571.
(51) Wong, H. C.; Coogan, R.; Intini, F. P.; Natile, G.; Marzilli, L. G. *Inorg. Chem.* **1999**, *38*, 777−787.
(52) Wong, H. C.; Intini, F. P.; Natile, G.; Marzilli, L. G. *Inorg. Chem.* **1999**, *38*, 1006−1014.
(53) Williams, K. M.; Cerasino, L.; Intini, F. P.; Natile, G.; Marzilli, L. G. *Inorg. Chem.* **1998**, *37*, 5260−5268.
(54) Carlone, M.; Fanizzi, F. P.; Intini, F. P.; Margiotta, N.; Marzilli, L. G.; Natile, G. *Inorg. Chem.* **2000**, *39*, 634−641.

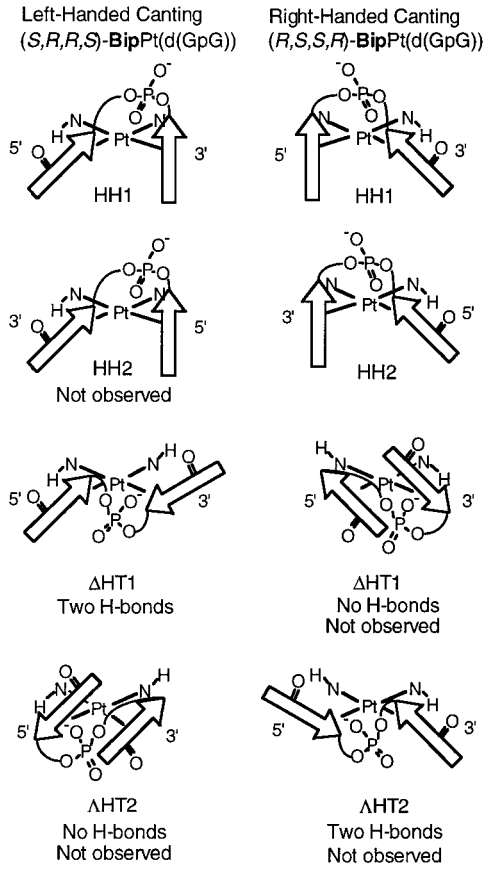

Figure 3. Schematic drawing showing the relationship of G O6 to **Bip** NH for conformers of **Bip**Pt(d(GpG)) adducts. In the HH forms, one G O6 could conceivably form an NH H-bond. In the HT forms, both G O6's or neither G O6 could form such an H-bond as indicated (see text).

tion of the phosphodiester backbone)[47] (Figure 3). Summarizing both **Bip**Pt(d(GpG)) studies,[34,47] we found that only four forms (HH1 R, HH1 L, HH2 R, and ΔHT1 L) were abundant. In all four, the **Bip** NH groups are on the correct side of the coordination plane to allow G O6−NH hydrogen bonding for at least one G. In each case, the canting observed permits such H-bonding. Molecular mechanics/dynamics (MMD) models gave some G O6−N distances of ∼2.7−3 Å,[34,47] consistent with the presence of hydrogen bonds.

The marked contrast between the findings for the **Bip**Pt(d(GpG)) adduct and the **Bip**Pt**G**$_2$ adducts (Chart 1) leads to two inter-related hypotheses: (1) the apparent hydrogen-bond interactions in the d(GpG) adducts result from the intrinsic structure of the conformers dictated by the dinucleotide and its N7 binding to Pt, and (2) such hydrogen bonding is not a driving force for the d(GpG) to adopt a particular structure.

To evaluate the influence of hydrogen bonding on d(GpG) adduct conformer stability and structure, we now have investigated the conformers formed by **Me$_2$ppz**Pt(d(GpG)) (**Me$_2$ppz** = *N*,*N*′-dimethylpiperazine, Figure 4). The absence of NH groups in the unusual **Me$_2$ppz** carrier ligand eliminates any influence of amine NH hydrogen bonding on conformer structure and distribution.[55,56] We also examine **Me$_2$ppz**Pt(GpG) here because GpG adducts provide valuable information for assessing the structure and properties of d(GpG) adducts.[35]

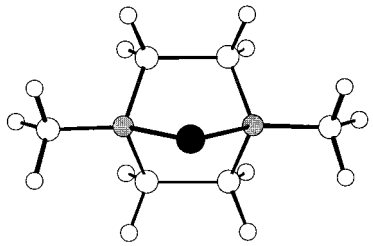

Figure 4. Ball-and-stick representation of the platinum moiety containing the ligand, **Me$_2$ppz**.

Experimental Section

Materials. Deoxyguanylyl(3′−5′)deoxyguanosine (d(GpG)) and guanylyl(3′−5′)guanosine (GpG) were purchased from Sigma. $PtCl_2$(**Me$_2$ppz**) was prepared as described.[55]

NMR Spectroscopy. All NMR samples (∼0.8 mM Pt) were prepared in D_2O at pH ∼4. $PtCl_2$(**Me$_2$ppz**) was treated with $AgNO_3$ (Pt:$AgNO_3$ ∼1:1.7) in the dark for ∼12 h to generate [**Me$_2$ppz**Pt$(D_2O)_2]^{2+}$. After AgCl was removed by filtration, 1 equiv (or slightly more) of d(GpG) or GpG was added. The sample was kept on ice for the early stages of the reaction. All spectra were collected on a Varian Inova 600 MHz instrument with a presaturation pulse to suppress the water peak, and the residual HOD resonance was used to reference ^{1}H NMR spectra. Saturation transfer experiments at 55 °C employed a presaturation pulse of 3 s and a pulse delay of 1 s. The appropriate symmetrical positions were irradiated, in addition to peaks of interest. Trimethyl phosphate was the ^{31}P NMR reference.

Nuclear Overhauser enhancement spectroscopy (NOESY), rotating frame Overhauser enhancement spectroscopy (ROESY), and correlation spectroscopy (COSY) data were collected at 5 °C with a spectral width of ∼6000 Hz in both dimensions, 256 or 512 blocks, 32−128 scans per block, and a 500 ms mixing time (NOESY and ROESY). Data were processed using an exponential apodization function with a line broadening of 1−3 Hz in t_2. Processing of t_1 employed a phase-shifted 90° sine bell function for NOESY and ROESY data and a squared sine bell function for COSY data. ^{1}H−^{31}P heteronuclear multiple bond correlation (HMBC) experiments were conducted at 5 °C using a spectral width of ∼1900 and ∼1700 Hz for the ^{1}H and ^{31}P dimensions, respectively, for 256 blocks, 48 scans per block. The data were processed using an exponential apodization function with line broadening in both dimensions. All NMR data (1D and 2D) were processed using the Felix 97.0 software.

Circular Dichroism (CD) Spectroscopy. Samples in water were ∼0.03 mM in d(GpG) or GpG. Spectra were collected from 400 to 200 nm at a scan speed of 50 nm/min on a JASCO J-600 CD spectropolarimeter; 10 scans were recorded and averaged for each sample.

High-Performance Liquid Chromatography (HPLC). Separations employed a Nucleosil C-18 reverse-phase column. Eluants A and B both contained 0.02 M ammonium acetate buffer, pH 5.5. Solvent A was water, and solvent B was a 70:30 methanol:water mixture. A flow rate of 2 mL/min was maintained over the course of a 60 min linear gradient (0 min = 95% A and 5% B, 60 min = 15% A and 85% B). Fractions were detected at 295 nm.

Molecular Mechanics and Dynamics (MMD). All MMD calculations were not restrained with NMR data and were carried out on a Silicon Graphics INDY R5000 workstation using the InsightII 97.0 software (MSI). The AMBER force field,[57] optimized for modeling of nucleic acids and related metal complexes,[58] was used in all modeling studies. Atomic charges and potential types for the **Me$_2$ppz** ligand are the same as those used in calculations for **Me$_2$ppz**Pt**G**$_2$ complexes.[56] Charges for platinated GpG and d(GpG) were determined as previously described.[58] Structures underwent 100 steepest-descent and 5000 conjugate-gradient iterations in energy minimizations. Structures were then subjected to dynamics simulation in which the temperature was

(55) Sullivan, S. T.; Ciccarese, A.; Fanizzi, F. P.; Marzilli, L. G. *Inorg. Chem.* **2000**, *39*, 836−842.
(56) Sullivan, S. T.; Ciccarese, A.; Fanizzi, F. P.; Marzilli, L. G. *Inorg. Chem.* **2001**, *40*, 455−462.
(57) Weiner, S.; Kollman, P. A.; Nguyen, D.; Case, D. *J. Comput. Chem.* **1986**, *7*, 230−252.
(58) Yao, S.; Plastaras, J. P.; Marzilli, L. G. *Inorg. Chem.* **1994**, *33*, 6061−6077.

Table 1. ^{1}H and ^{31}P NMR Signals (ppm) for **Me$_2$ppz**Pt(d(GpG)) and **Me$_2$ppz**Pt(GpG)[a]

conformer (%)	G[b]	H8	H1′	H2′	H2″	$J_{H1'-H2'}/J_{H1'-H2''}$	H3′	H4′	base sugar[c]	^{31}P
					Me$_2$ppz Pt(d(GpG))					
HH1 (50%)	5′	8.51	6.16	2.42	2.73	0/7.6 (d)	5.01	4.05	anti	−2.89
	3′	8.93	6.21	2.50	2.40	10.0/4.9 (dd)	4.63	4.15	anti	
HH2 (20%)	5′	8.71	6.15	3.01	2.77	0/7.5 (d)	4.83	4.05	anti	−2.20
	3′	8.78	6.11	2.12	2.61	9.1/5.0 (dd)	4.60	4.38	anti	
ΔHT1 (30%)	5′	7.78	6.08	2.83	2.47	0/6.3 (d)		4.00	anti	−5.12
	3′	7.90	6.00	3.25	2.41	3.1/8.5 (dd)	4.92	3.97	syn	
					Me$_2$ppz Pt(GpG)					
HH1 (86%)	5′	8.62	5.93	4.22		0 (s)	4.81	4.25	anti	−3.18
	3′	8.78	5.83	4.42		8.2 (d)	4.33	4.23	anti	
ΔHT1 (14%)	5′	7.86	5.82	4.53		0 (s)	3.54	4.14	anti	−4.88
	3′	7.91	5.64	5.15		2.2 (d)	4.94	4.04	syn	

[a] 2D experiments conducted at 5 °C, pH ∼4.0. [b] 5′-G, 3′-G assignments based on ^{1}H−^{31}P coupling data from HMBC experiment. [c] Anti/syn conformational assignment based on relative strength of NOE cross-peaks between H8 resonances and H1′ or H2′/H2″ signals.

raised to 300 K. Steepest-descent and conjugate-gradient minimizations were carried out for 200 and 500 000 iterations, respectively, and the 50 lowest-energy conformations were collected.

Results

Conformer Assignment and Conformational Features. For the **Me$_2$ppz**Pt(dinucleotide) adducts [dinucleotide = d(GpG) or GpG], NOESY, COSY, ^{1}H−^{31}P HMBC, and (for d(GpG) only) ROESY data were used to assign H8 and sugar proton signals (Table 1; please see Supporting Information for details of the assignment method). These methods were used to assess structure. For example, in addition to characteristic H1′ coupling patterns associated with S- and N-sugar pucker conformations, H8−H3′ NOE cross-peaks are characteristically observed for N-sugars.[59,60] In such adducts, the sugar residue of the 5′-G typically adopts an N-pucker conformation.[19,47,61] G nucleotide conformations can be distinguished by examination of H8-sugar signal NOE cross-peaks; observation of strong H8−H2′/H2″ NOE cross-peaks and weak (or unobservable) H8−H1′ cross-peaks are characteristic of an anti conformation, while strong H8−H1′ NOEs are typically found for syn residues.[60,62,63] G residues of *cis*-PtA_2(dinucleotide) HH forms typically retain the anti conformation found in B-DNA.[18,19,21,47] HH and HT base arrangements are best assessed through H8−H8 NOE cross-peaks; such a cross-peak is characteristic of an HH form, whereas the absence of such a cross-peak is indicative of an HT form because the H8 atoms are closer in the HH forms compared to the HT conformers.[34,47] HH and HT forms of *cis*-PtA_2(d(GpG))/*cis*-PtA_2(GpG) complexes often give rise to characteristic NMR signal shifts; HH forms typically exhibit H8 and ^{31}P signals more downfield than those of the free d(GpG)/GpG dinucleotide,[18,19,46,64−66] whereas HT conformers have been found to have more upfield-shifted H8 and ^{31}P NMR signals.[34,35] Key observations related to conformational features of **Me$_2$ppz**Pt(dinucleotide) adducts are discussed below.

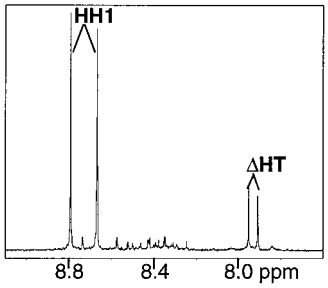

Figure 5. H8 region of **Me$_2$ppz**Pt(GpG) 1D NMR spectrum, collected at room temperature, pH 3.7, in D_2O.

Me$_2$ppzPt(GpG). We present the results for the GpG adduct first because it adopts one fewer conformation than the d(GpG) adduct. After addition of 1 equiv of GpG to a D_2O solution of [**Me$_2$ppz**Pt$(D_2O)_2$]$^{2+}$ (pH ∼4), a dominant set of two H8 resonances, arising from an HH form (see below), was observed at 30 min. At ∼2.5 h, a smaller, upfield set of H8 signals of an HT form was observed. When this reaction was monitored with time, no changes in conformer distribution were observed after 1 week (amounts of HH and HT conformers were 86% and 14%, respectively, Figure 5); thus, this is the equilibrium distribution at room temperature. Platination at N7 was established by the absence of shift changes for these four dominant H8 signals as the pH was lowered to 1.3. ^{31}P NMR signals at −3.18 and −4.88 ppm were assigned to the HH and HT forms, respectively, on the basis of their relative intensities. Several minor species, in amounts too small to characterize, were also observed during the course of the reaction and persisted after reaction completion.

Saturation transfer experiments at 55 °C showed no transfer of magnetization between the observed H8 signals. Also, the chemical shifts of the H8 signals were largely temperature independent. However, the conformer distribution was found to be temperature sensitive. After 3 days at 60 °C, the relative HH:HT percentages changed from 86:14% to 57:43%. (Heating beyond this time resulted in the loss of H8 signals because of exchange with solvent deuterium.)

As the pH was raised from ∼4 to ∼10, three of the four H8 signals shifted slightly upfield (∼0.2−0.3 ppm). Relatively little change in the HH and HT distribution was observed initially. However, after 8 days at pH ∼10, the relative percentages of the HH and HT forms were 63% and 37%, respectively. (Some of the minor signals present at reaction completion increased slightly at this high pH, but the signals were still too small to allow characterization of the forms.) After the pH was lowered again to ∼4, the conformer distribution slowly changed toward the low pH equilibrium distribution (Supporting Information).

(59) Saenger, W. *Principles of Nucleic Acid Structure*; Springer-Verlag: New York, 1984; pp 1−556.
(60) Wuthrich, K. *NMR of Proteins and Nucleic Acids*; John Wiley & Sons: New York, 1986.
(61) Sherman, S. E.; Gibson, D.; Wang, A. H.-J.; Lippard, S. J. *Science* **1985**, *230*, 412−417.
(62) Kaspárková, J.; Mellish, K. J.; Qu, Y.; Brabec, V.; Farrell, N. *Biochemistry* **1996**, *35*, 16705−16713.
(63) Patel, D. J.; Kozlowski, S. A.; Nordheim, A.; Rich, A. *Proc. Natl. Acad. Sci. U.S.A.* **1982**, *79*, 1413−1417.
(64) den Hartog, J. H. J.; Altona, C.; van der Marel, G. A.; Reedijk, J. *Eur. J. Biochem.* **1985**, *147*, 371−379.
(65) van der Veer, J. L.; van der Marel, G. A.; van den Elst, H.; Reedijk, J. *Inorg. Chem.* **1987**, *26*, 2272−2275.
(66) Mukundan, S., Jr.; Xu, Y.; Zon, G.; Marzilli, L. G. *J. Am. Chem. Soc.* **1991**, *113*, 3021−3027.

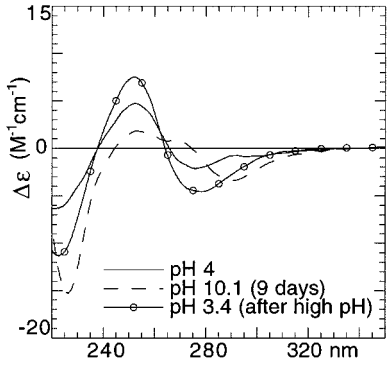

Figure 6. **Me$_2$ppz**Pt(GpG) CD spectra collected in water at low pH (∼4) and room temperature (reflecting low pH equilibrium conformer distribution), after sample kept at high pH (∼10) for 9 days (high pH conformer distribution), and then immediately after pH was lowered to 3.4 (high pH conformer distribution at low pH).

The CD signal for **Me$_2$ppz**Pt(GpG) also exhibited a pH dependence. Immediately after a pH adjustment from ∼4 to ∼10, a weaker CD signal with a shifted lower energy feature was observed. This signal, with negative and positive features at ∼290 and ∼250 nm, respectively, increased for 9 days. No changes were observed after this time (Figure 6). The pH was then lowered to ∼3, and the CD spectrum was recorded immediately. The resulting signal was similar in shape but more intense than the signal collected before the pH was raised (Figure 6).

Conformational Features of Me$_2$ppzPt(GpG) Conformers. The upfield pair of H8 signals (7.86, 7.91 ppm) observed for **Me$_2$ppz**Pt(GpG) has no H8−H8 NOE cross-peak, indicating that the bases of this form adopt the HT arrangement.[34,35,47] Also, the upfield shift position of these signals is characteristic of HT forms.[34,35] The more upfield H8 peak exhibited an intraresidue H8−H3′ NOE cross-peak. This finding, along with the absence of any observable coupling for the H1′ resonance of this residue, is consistent with an N-sugar pucker.[59,60] This residue is unambiguously the 5′-G because its H3′ resonance is coupled to the ^{31}P NMR signal of this form in the ^{1}H−^{31}P HMBC spectrum. (In such an experiment with nucleic acids, H3′−^{31}P coupling is observed for the 5′-residue, while H4′/H5′/H5″−^{31}P coupling is found for the 3′-residue.[67,68]) The absence of an H8−H1′ NOE cross-peak suggests that this 5′-G is anti.[60,62,63] The observation of an intraresidue H8−H1′ NOE cross-peak for the more downfield H8 signal of this HT form (which, by default, must be the 3′-G H8) suggests that the conformation of the 3′-G is syn.[60,62,63] This 3′-G H1′ signal is a doublet and is characteristic of an S-sugar pucker.[59] However, the small $^{3}J_{H1'-H2'}$ value (2.2 Hz) observed for this H1′ signal suggests that this sugar residue is not strictly S but possesses some N character as well.[18] These observations are consistent with an *anti*,*syn*-HT form. Two HT conformations (Δ and Λ, Figure 3) are possible. The CD signal exhibited by **Me$_2$ppz**Pt(GpG) (with negative and positive features at ∼280 and ∼250 nm, respectively, Figure 6) is similar in shape to that found for ΔHT conformers of *cis*-PtA_2**G**$_2$ complexes[43,51−53] and for the ΔHT1 form of (*S*,*R*,*R*,*S*)-**Bip**Pt(GpG).[35] Therefore, the HT form observed for **Me$_2$ppz**Pt(GpG) is assigned the Δ chirality. (Respectively, the ΔHT and ΛHT forms have the same and opposite phosphodiester backbone propagation direction as the normal HH1 form, Figure 3; thus, these are designated as ΔHT1 and ΛHT2.)

Table 2. Summary of Lowest-Energy Models Generated from Unrestrained MMD Calculations for **Me$_2$ppz**Pt(d(GpG)) and **Me$_2$ppz**Pt(GpG) Conformers

complex	conformer	energy (kcal/mol)	syn G[a]
Me$_2$ppz Pt(d(GpG))	HH1	25.29	
	HH2	22.95	
	ΔHT1	24.78	3′-G
	ΛHT2	20.24	3′-G, 5′-G
Me$_2$ppz Pt(GpG)	HH1	25.28	
	HH2	23.73	
	ΔHT1	25.21	3′-G
	ΛHT2	20.66	3′-G, 5′-G

[a] Determination of syn G residue based on χ angle (C4−N9−C1′−O4′) values (typically between −90° and 90°) and H8−H1′ distances (≤3 Å).

When the ΔHT1 model was minimized by MMD calculations, the lowest-energy structure had an *anti*-5′-G and *syn*-3′-G (Table 2), in agreement with experimental results. In contrast, an energy-minimized *anti*,*syn*-ΛHT structure could not be generated; the lowest-energy model had a *syn*,*syn*-ΛHT structure (Table 2). Similar MMD results were reported previously.[34,35] For (*S*,*R*,*R*,*S*)-**Bip**Pt(GpG), the HT form present at pH ∼7 and below was the *anti*,*syn*-ΔHT conformer.[35] In that study, a possible ΛHT2 form was found but only under high pH (∼10) conditions.[35] The ΛHT2 form, which has a CD signal opposite in sign to that of the ΔHT1 form, is possibly stabilized by two amine NH−G O6 hydrogen bonds (made strong by G N1H deprotonation);[35] such stabilizing forces are not possible in **Me$_2$ppz**Pt(dinucleotide) adducts. In summary, the observed HT form of **Me$_2$ppz**Pt(GpG) is clearly indicated by CD data to be the ΔHT1 form; the NMR data establish that the form has an *anti*,*syn*-HT conformation, and the MMD calculations show that the ΔHT1 form favors an *anti*,*syn* conformation.

The dominant H8 signals arise from an HH form because an H8−H8 NOE cross-peak was observed.[34,47] The 8.62 ppm H8 signal has H2′ and H3′ but not H1′ intraresidue NOE cross-peaks. The H1′ signal is a singlet. These observations are consistent with an anti residue and N-sugar pucker.[59,60,62,63] The signals are assigned to the 5′-G because this residue's H3′ resonance has a ^{31}P−^{1}H HMBC cross-peak.[67,68] The 8.78 ppm H8 signal, which must be the 3′-G H8 signal, has an NOE cross-peak to its respective H2′ sugar signal. This observation, along with the absence of an observable H8−H1′ NOE cross-peak, is consistent with an anti G,[60,62,63] which is typically observed for HH forms of *cis*-PtA_2(dinucleotide) complexes.[18,19,21,47] Because the H1′ signal exhibited the coupling pattern characteristic of this conformation, the sugar moiety of this 3′-G residue has the S-pucker conformation.[59] The two possible *anti*,*anti*-HH conformers, HH1 or HH2, differ only in the directions of phosphodiester backbone propagation[47] and thus exhibit few spectral differences. The initial discovery of the HH2 form involved **Bip**Pt(dinucleotide) adducts; the difference in the residue with the canted base provided a clear way to distinguish between the HH forms. Canting, however, is not significant for **Me$_2$ppz**Pt(GpG). Another, less obvious spectral difference between the HH forms is the absence of any observable H8-sugar NOESY cross-peaks for the 3′-G of the HH2 form, whereas the HH1 conformer has such cross-peaks.[47,69] Thus, the presence of an H8−H2′ NOE for the 3′-G of this HH form, combined with past studies of **Bip**Pt(GpG) adducts indicating

(67) Gotfredsen, C. H.; Meissner, A.; Duus, J. O.; Sorensen, O. W. *Magn. Reson. Chem.* **2000**, *38*, 692−695.
(68) Qu, Y.; Bloemink, M. J.; Reedijk, J.; Hambley, T. W.; Farrell, N. *J. Am. Chem. Soc.* **1996**, *118*, 9307−9313.
(69) Saad, J.; Marzilli, L. G., unpublished work, 2001.

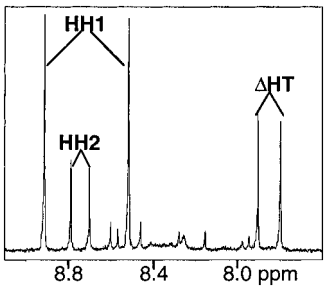

Figure 7. H8 region of **Me$_2$ppz**Pt(d(GpG)) 1D NMR spectrum, pH 4.0, collected at room temperature in D_2O.

that the HH2 conformer is highly disfavored in GpG adducts,[35] leads us to believe that the **Me$_2$ppz**Pt(GpG) HH form is undoubtedly HH1.

Me$_2$ppzPt(d(GpG)). Soon after the addition of 1 equiv of d(GpG) to a dilute D_2O solution of [**Me$_2$ppz**Pt$(D_2O)_2$]$^{2+}$ (pH ∼4), two new pairs of H8 signals were observed. These resonances, of roughly equal intensity, arise from HH forms because these H8 signals have downfield shifts and each pair is connected by H8−H8 NOEs (see below). After ∼1 h, a third, smaller pair of H8 signals was observed upfield of the other two pairs. Because no NOE cross-peak connected these H8 signals, these upfield H8 resonances arise from an HT form. The equilibrium distribution, reached after 1 week at room temperature, was 50%, 20%, and 30% for the two HH forms and the HT form, respectively (Figure 7). Platination at N7 was confirmed by lowering the pH, as described for the GpG adduct. ^{31}P NMR signals were found at −2.20, −2.89, and −5.12 ppm for the **Me$_2$ppz**Pt(d(GpG)) complex; from their relative intensities, these signals were assigned to the minor HH form, the dominant HH form, and the HT conformer, respectively. Minor forms, in amounts too small to permit characterization, were observed over the course of the reaction and upon reaction completion.

The H8 signals of the three major forms did not shift significantly between 25 and 55 °C. Saturation transfer experiments revealed no transfer of magnetization between H8 signals at 55 °C. After 2 days at 60 °C, a change in the distribution was observed (54%, 11%, and 35% for the two HH forms and the HT form, respectively). (Further distribution changes with heating could not be monitored because of the loss/exchange of the H8 signals.)

No distribution changes were observed as the pH was raised from ∼4 to ∼7. As the pH was raised from ∼7 to ∼10, five of the six H8 signals shifted upfield (Supporting Information), and no immediate changes were observed in conformer distribution. However, after 6 days at pH ∼10, the amount of the HT conformer had increased significantly, while the amounts of both HH forms decreased. Further changes were noted up to 9 days, at which time the relative conformer distribution was found to be 38%, <1%, and 62% for the two HH forms and HT conformer, respectively. As found for the GpG adduct, the signals of minor species found at reaction completion were observed to grow slightly at this high pH of ∼10. Allowing the sample to sit at low pH (∼3) for 11 days restored the conformer distribution to one similar to that observed upon completion of the [**Me$_2$ppz**Pt$(D_2O)_2$]$^{2+}$+ d(GpG) reaction (Supporting Information).

The CD signal of the **Me$_2$ppz**Pt(d(GpG)) complex also exhibited a pH dependence; this dependence was similar to that observed for the **Me$_2$ppz**Pt(GpG) adduct. When the pH was raised to ∼10, a weaker signal with the low-energy feature shifted to a longer wavelength was observed (negative and positive features at ∼290 and ∼250 nm, Figure 8). The intensity of this signal changed with time; no changes were noted after 9 days. The pH was then lowered to ∼3, and the CD spectrum was immediately collected. The resulting spectrum was similar in shape to that observed upon reaction completion but exhibited more intense signals (Figure 8).

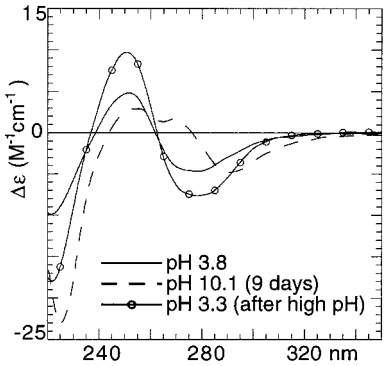

Figure 8. **Me$_2$ppz**Pt(d(GpG)) CD spectra collected in water at low pH (∼4) and room temperature (reflecting low pH equilibrium conformer distribution), after sample kept at high pH (∼10) for 9 days (high pH conformer distribution), and then immediately after pH was dropped to 3.3 (high pH conformer distribution at low pH).

The three forms of **Me$_2$ppz**Pt(d(GpG)) were separated by HPLC. All three peaks were again observed when each collected fraction was re-injected onto the HPLC column 1 week after initial collection. With time, signals of all conformers were observed in CD spectra and ^{1}H NMR spectra of each of the fractions. These observations prove that these forms must be conformers that re-equilibrate.

Conformational Features of Me$_2$ppzPt(d(GpG)) Conformers. For the **Me$_2$ppz**Pt(d(GpG)) HT form, the 7.78 ppm H8 signal lacked an H8−H1′ NOE cross-peak but had an H8−H2′ NOE cross-peak, consistent with a G residue having an anti conformation.[60,62,63] The coupling pattern of the H1′ signal of this residue is consistent with an N-sugar pucker;[59] such puckering is commonly found for the 5′-G residue of a cross-link.[19,47,61] Furthermore, the signals of the other residue are consistent with the 3′-G. In particular, H4′/H5′/H5″−^{31}P coupling, characteristic of a 3′-residue, was found for the G moiety with the 7.90 ppm H8 signal.[67,68] The H8−H1′ NOE cross-peak observed for the 3′-G demonstrates that this residue is syn.[60,62,63] The doublet of doublets coupling pattern observed for the H1′ resonance is characteristic of an S-sugar pucker;[59] however, the relatively small (3.1 Hz) $^3J_{H1'-H2'}$ value suggests that the 3′-G sugar moiety has some N character.[18] (The ROESY data, Supporting Information, support the conclusions drawn from the NOESY data. The 5′-G H3′ signal could not be assigned, most probably because it comes at the same shift as the HOD peak.) This *anti*,*syn*-HT form is assigned the Δ chirality because the CD signal exhibited by **Me$_2$ppz**Pt(d(GpG)) (nearly identical to that of **Me$_2$ppz**Pt(GpG)) has the characteristic ΔHT shape (Figure 8).[35,43,51−53] The ΔHT1 model minimizes with a 5′-G anti, 3′-G syn conformation consistent with the experimental results. In contrast, the ΛHT2 model minimized with both G's syn, a model inconsistent with both the CD and the NMR data (see Table 2 and ref 35).

For the dominant **Me$_2$ppz**Pt(d(GpG)) form, which showed an H8−H8 NOE, the 8.51 ppm H8 signal had NOE cross-peaks to H2′/H2″ signals; these cross-peaks and the absence of an H8−H1′ cross-peak in the NOESY spectrum are consistent with an anti G.[60,62,63] The H1′ signal of this residue is a doublet, characteristic of an N-pucker for a deoxyribose sugar.[59] The

observed H8−H3′ NOE cross-peak confirms the N-sugar pucker.[60] These signals are therefore assigned to the 5′-G.[19,47,61] This assignment is confirmed by the $^{1}H-^{31}P$ HMBC cross-peak observed for the H3′ signal of this residue. The 8.93 ppm H8 signal, which must be the 3′-G H8 signal, had H8−H2′/H2″ cross-peaks but no H8−H1′ cross-peak in the NOESY spectrum, indicating an anti G.[60,62,63] The doublet of doublets coupling of the 3′-G H1′ signal is typical of an S-sugar.[59] (ROESY data also agree with the *anti,anti*-HH conformation deduced from the NOESY data. In contrast to the NOESY spectrum, the ROESY spectrum, Supporting Information, showed H8−H1′ cross-peaks; their weak intensity, relative to the observed H8−H2′/H2″ cross-peaks, is consistent with the anti conformation.) Thus, both NOESY and ROESY data confirm that the dominant form is an *anti,anti*-HH form.

The H8 signals for the third most abundant **Me$_2$ppz**Pt(d(GpG)) species are small and not well dispersed, making it difficult to determine whether the "cross-peak" in the NOESY spectrum is a true cross-peak or simply the result of noise. However, a 1D NOE was observed between these two H8 signals at 5 °C (Supporting Information), thereby confirming the HH arrangement of the bases.[34,47] The 8.71 ppm H8 signal had an NOE cross-peak to H2′ but not to H1′ in the NOESY spectrum; these observations are characteristic of the anti conformation.[60,62,63] Also, this resonance has an H8−H3′ NOE, a finding typical for N-sugars.[60] The coupling pattern of the H1′ signal of this residue also is consistent with an N-sugar pucker.[59] This residue was assigned to the 5′-G because the H3′ resonance has a $^{1}H-^{31}P$ HMBC cross-peak. Monitoring the formation reaction with time allowed assignment of a doublet of doublets as the 3′-G H1′ signal; this coupling pattern is characteristic of an S-sugar pucker.[59] The absence of any observable H8−H1′ NOE for this residue establishes that it is anti.[60,62,63] (Again, the ROESY data agree with these assignments, Supporting Information.) This form, then, is also an *anti,anti*-HH form.

The observation of two *anti,anti*-HH forms is in agreement with unrestrained MMD calculations, which suggest that the HH1 and HH2 forms are both likely to be present in detectable amounts because they differ by only ∼2 kcal/mol.[47] Distances between the H8 atom and sugar protons of the 3′-G residue for the lowest-energy HH2 structure indicate that observable NOEs are unlikely. No H8-sugar cross-peaks were identified for the 3′-G H8 signal (8.78 ppm) in the NOESY spectrum. A similar result was found for the HH2 form of (*R,S,S,R*)-**Bip**Pt(d(GpG))[47] and (*R,R*)-**Me$_4$DAB**Pt(d(GpG))[69] (**Me$_4$DAB** = *N,N,N′,N′*-tetramethyl-2,3-diaminobutane). This result and assessments of chemical shifts (Supporting Information) and CD spectra (see below) support the assignment of the major and minor HH forms to HH1 and HH2, respectively.

Separation of the three conformers by HPLC allowed observation of the individual CD signal of each form (Figure 9). Although of weak intensity, the two HH forms exhibit markedly different CD signals from one another; the HH1 form exhibited negative and positive features at ∼280 and ∼250 nm, respectively, while the CD signal for HH2 form was nearly opposite to that of HH1, with positive and negative features at ∼280 and ∼250 nm, respectively (Figure 9). Thus, we deconvoluted the CD spectra for the **Me$_2$ppz**Pt(GpG) HH1 and ΔHT1 conformers (Figure 10), by the method reported for **Bip**Pt(d(GpG)) and **Bip**Pt(GpG) adducts,[35] in order to compare the calculated **Me$_2$ppz**Pt(GpG) HH1 CD signal to those observed for the two HH forms of **Me$_2$ppz**Pt(d(GpG)). The calculated CD signal for the **Me$_2$ppz**Pt(GpG) HH1 conformer was, as expected, weak with a slightly negative feature at ∼280 nm and a positive band at ∼250 nm (Figure 10). This comparison indicates that the dominant **Me$_2$ppz**Pt(d(GpG)) HH form is HH1. Thus, NMR shift and CD signal comparisons add further support to the 2D NMR data and indicate that the dominant HH form has the HH1 conformation.

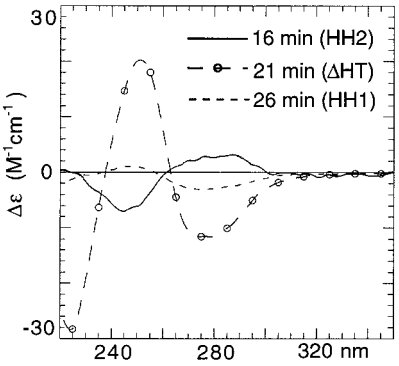

Figure 9. CD spectra of individual **Me$_2$ppz**Pt(d(GpG)) HPLC fractions recorded immediately after fraction collection.

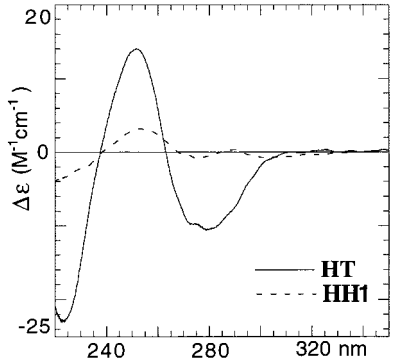

Figure 10. Deconvoluted CD signals for the ΔHT1 (solid line) and HH1 (dotted line) conformers of **Me$_2$ppz**Pt(GpG) in water at room temperature.

Discussion

In contrast to very bulky carrier ligands such as *N,N,N′,N′*-tetramethylethylenediamine used previously to eliminate the dynamic motion problem,[36] the **Me$_2$ppz** and **Bip** ligands were designed to permit formation of (carrier ligand)Pt**G**$_2$ and (carrier ligand)Pt(dinucleotide) adducts, allowing the coexistence of multiple conformers. The bulk in the designed ligands is located in a position that destabilizes the transition state for rotation about the Pt−G N7 bond. In the ground state, clashes between the G O6 atoms and the carrier ligand moieties are kept low. The **Me$_2$ppz** carrier ligand is unique for an sp^3 N-donor diamine in that its significant bulk is essentially in the coordination plane. Also, **Me$_2$ppz** lacks NH groups. Consequently, forces within the Pt(dinucleotide) moiety itself should dictate conformation. We hoped to assess this concept by comparing the **Me$_2$ppz**Pt and **Bip**Pt adducts. If the conformation found for a given corresponding conformer were similar or identical, this finding would be unambiguous evidence that hydrogen bonding is weak or nonexistent. However, if the conformers differed, insight would be gained into carrier ligand effects. As discussed below, this comparison of conformers of **Me$_2$ppz**Pt and **Bip**Pt dinucleotide adducts indicates the following: (i) the backbone is nearly independent of carrier ligand effects for a given conformer; (ii) the structure of the ΔHT1 form is minimally influenced by the carrier ligand; and (iii) base canting of the HH forms and, as a

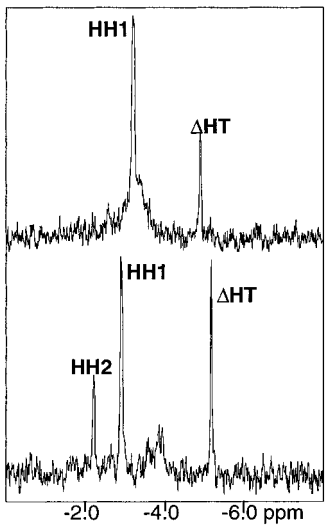

Figure 11. ^{31}P NMR spectra of **Me$_2$ppz**Pt(GpG), pH 3.8 (top), and **Me$_2$ppz**Pt(d(GpG)), pH 3.6 (bottom), recorded in D_2O at room temperature.

consequence, relative conformer stability are dependent on the carrier ligand.

Comparison of the Sugar Phosphodiester Backbone of Me$_2$ppzPt(dinucleotide) and *cis*-PtA$_2$(dinucleotide) Conformers. The 5′-G of all conformers of the **Me$_2$ppz**Pt(dinucleotide) adducts was found to adopt the N-sugar pucker, a feature found universally in such cross links.[17,47,65,66] Thus, the favored 5′-G sugar conformation appears to be independent of the carrier ligand. Likewise, the 3′-G sugar of HH conformers of **Me$_2$ppz**Pt(dinucleotide) adducts, as generally found for all cross-link adducts including the nondynamic **Bip**Pt(dinucleotide) adducts,[34,35,47] retains the S conformation favored by the free nucleic acid derivative. In addition, the ΔHT1 forms of all nondynamic adducts have mainly a 3′-G S sugar, but this sugar has some N character. Finally, the structure-sensitive ^{31}P NMR chemical shifts observed for the conformers of **Me$_2$ppz**Pt(d(GpG)) (Figure 11) agree with those for the corresponding conformer of **Bip**Pt(dinucleotide) adducts.[34,47] This similarity of the ^{31}P NMR data, combined with the ^{1}H NMR data on sugar pucker, leaves little doubt that the sugar phosphodiester backbone structure is not influenced by the carrier ligand, although the backbone does differ from conformer to conformer, as expected.

Base Canting. The second most significant parameter involving the G bases, after the HH or HT orientation, is base canting. The G bases do not lie exactly perpendicular to the coordination plane, and the degree and the direction (left- or right-handed, Figure 3) of canting differ depending on the carrier ligand, the presence or absence of a linkage between the bases, the sugar (ribo or deoxyribo), the presence or absence of a flanking residue, and even the single-stranded or duplex character of the DNA. Fortunately, canting can be assessed in a semiquantitative fashion by using the H8 shift.[34] For a canted G base (see below), the H8 experiences the upfield shifting effect of the ring-current anisotropy of the other cis base.[21] In an uncanted base, the H8 atom is positioned away from the G base and closer to the *z* axis of the heavy platinum atom; as a result, the H8 signal should be downfield because there is less shielding by the cis G and possibly greater deshielding by the anisotropic Pt atom.[54,56,70,71]

(70) Elizondo-Riojas, M.-A.; Kozelka, J. *Inorg. Chim. Acta* **2000**, *297*, 417−420.

(71) Sundquist, W.; Lippard, S. J. *Coord. Chem. Rev.* **1990**, *100*, 293−322.

Base Canting and Structure of the ΔHT1 Conformer. In the most recent version of the H8 shift method for assessing canting, H8 shifts of ∼7.8 ppm are proposed to be indicative of a highly canted G base.[34] By this criterion, both the 3′- and the 5′-G residues of the ΔHT1 conformer of the **Me$_2$ppz**Pt(dinucleotide) adducts have a canted G base. Two types of shift evidence indicate that the G bases in this ΔHT1 form of these adducts undoubtedly cant in an almost identical manner as in the ΔHT1 form of the (*S*,*R*,*R*,*S*)-**Bip**Pt(dinucleotide) adducts. *First*, the H8 shifts exhibited by the ΔHT1 conformer of **Me$_2$ppz**Pt(dinucleotide) (Table 1) and (*S*,*R*,*R*,*S*)-**Bip**Pt(dinucleotide) adducts are similar [7.77 and 7.91 ppm for 5′- and 3′-G H8, respectively, of (*S*,*R*,*R*,*S*)-**Bip**Pt(d(GpG)), 7.84 and 7.96 ppm for 5′- and 3′-G H8, respectively, of (*S*,*R*,*R*,*S*)-**Bip**Pt(GpG)].[34,35] *Second*, for the **Me$_2$ppz**Pt(dinucleotide) and (*S*,*R*,*R*,*S*)-**Bip**Pt(dinucleotide) adducts, the 5′-G and 3′-G H8 signals of the ΔHT1 form shift upfield ∼0.30 and ∼0.20 ppm, respectively, from pH ∼4 to ∼10.[35] Carrier ligand NH group−G O6 hydrogen bonds are stronger after N1H deprotonation. The hydrogen bonding is facilitated by a more canted G base. More upfield-shifted H8 signals, indicative of greater base canting, would be expected for the ΔHT1 form of (*S*,*R*,*R*,*S*)-**Bip**Pt(dinucleotide) adducts, relative to that for the ΔHT1 form of **Me$_2$ppz**Pt(dinucleotide) adducts, if such interactions were a prominent stabilizing force. Instead, these similar upfield shift changes observed for the ΔHT1 H8 signals simply reflect N1H deprotonation. These two types of findings suggest that (a) G base canting for the ΔHT1 form is not influenced by carrier ligand−G O6 hydrogen bonds but is governed by the dinucleotide itself, and (b) carrier ligand−G O6 hydrogen bonds are not present in the ΔHT1 form of the (*S*,*R*,*R*,*S*)-**Bip**Pt(dinucleotide) adducts. This second statement is also supported by the evidence discussed below that N1H deprotonation increases the stability of the ΔHT1 form of dinucleotide adducts containing either the (*S*,*R*,*R*,*S*)-**Bip** or the **Me$_2$ppz** carrier ligand. For (*S*,*R*,*R*,*S*)-**Bip**Pt(dinucleotide) adducts, the conclusion is clear that the ΔHT1 form is not influenced structurally by such hydrogen bonding.

Base Canting and Structure of the HH Conformers. In the same H8 shift method for assessing canting mentioned above, an uncanted G base in a d(GpG) adduct has an H8 signal with a shift of ∼9.0 (3′-G) or ∼8.7 (5′-G) ppm. For the **Me$_2$ppz**Pt(d(GpG)) and **Me$_2$ppz**Pt(GpG) HH conformers, the H8 shift values (between ∼8.8 and ∼8.9 ppm, and between ∼8.5 and ∼8.7 ppm for the 3′-G and 5′-G, respectively) are consistent with two uncanted bases. This is unusual because in almost every other case, one base of an HH form is canted. For example, in contrast to the ΔHT1 form, the H8 shifts exhibited by the HH1 and HH2 forms of **Me$_2$ppz**Pt(dinucleotide) adducts differ from those exhibited by the analogous HH forms for the d(GpG)/GpG adducts with the **Bip** carrier ligand. These forms have one canted base (Figure 3).

The H8 signal for the more canted base of all HH forms of the **Bip**Pt(d(GpG)) and **Bip**Pt(GpG) adducts was found to undergo a greater upfield shift between pH ∼4 and pH ∼10 than the less canted base; this finding is consistent with greater base canting to facilitate carrier ligand NH group−G O6 hydrogen bonds after N1H deprotonation.[35] In comparison, less pronounced H8 shift changes, as a function of pH, were found for all H8 signals of **Me$_2$ppz**Pt(dinucleotide) HH1 and HH2 conformers (Supporting Information), consistent with the absence of canting. The different H8 chemical shifts of the corresponding HH forms of **Me$_2$ppz**Pt and **Bip**Pt dinucleotide adducts demonstrate that bases in these HH forms have different

canting. Although for **Bip**Pt adducts either steric effects of the piperidine rings or very weak carrier ligand−G O6 hydrogen bonds could influence canting, we believe steric effects are more important for reasons to be discussed below. In any case, the conclusion is clear that, for any given HH conformer, the **Bip** carrier ligand can in some cases influence base canting, but it does not greatly influence the sugar phosphate backbone.

Factors Influencing Conformer Distribution. Three of the four possible conformers were found to be abundant for **Me$_2$ppz**Pt(d(GpG)). However, only two of these forms were abundant at equilibrium for each **Bip**Pt(d(GpG)) adduct (HH1 and HH2 for (*R*,*S*,*S*,*R*)-**Bip**Pt(d(GpG)), and HH1 and ΔHT1 for (*S*,*R*,*R*,*S*)-**Bip**Pt(d(GpG))).[34,47] The different forms reported for the cross-linked models with the two different **Bip** configurations demonstrate that the stereochemistry of the **Bip** carrier ligand influences which conformers are formed and favored. Hydrogen-bonding interactions between the amine NH groups and the O6's of the d(GpG) moiety are possible in all forms and could conceivably help stabilize the observed forms.[34,47] However, it appears to be more likely that the piperidine rings, forcing as they do a particular handedness in the base canting, sterically influence the conformer distribution. The HH1 form can be either right- or left-handed and thus is found in all cases (Figure 3). However, it is clear that the ΔHT1 conformer cannot be accommodated well in the (*R*,*S*,*S*,*R*)-**Bip**Pt(dinucleotide) adducts, which have only R canting. Likewise, the HH2 form prefers R canting and is not one of the abundant (*S*,*R*,*R*,*S*)-**Bip**Pt(d(GpG)) conformers, which favor L canting.

Although the **Me$_2$ppz** ligand does not limit d(GpG) conformations as much as the **Bip** ligands do, neither the (*R*,*S*,*S*,*R*)-**Bip**Pt nor the **Me$_2$ppz**Pt GpG adduct adopts the HH2 conformation. Thus, assuming we are correct about the minimal effect of the **Me$_2$ppz** carrier ligand on dinucleotide conformation, an HH2 form appears to be unfavorable in GpG cross-link models because of an inherent feature of the Pt(GpG) macrocyclic ring. The cause of this instability of the GpG ligand in the HH2 conformation is unclear, but it must lie in the type of sugar moiety, which is the only difference between GpG and d(GpG).

The ΔHT1 conformer of the **Me$_2$ppz**Pt(dinucleotide) adducts becomes favored upon N1H deprotonation (pH >9). More favorable amine−G O6 hydrogen bonding upon N1H deprotonation was offered as a possible explanation for the related pH-dependent increase in the ΔHT1 form of the (*S*,*R*,*R*,*S*)-**Bip**Pt(dinucleotide) adducts.[35] However, this explanation cannot account for the increase of the **Me$_2$ppz**Pt(dinucleotide) ΔHT1 form because there are no carrier ligand NH groups. N1H deprotonation favors the HT arrangement for some other reason, possibly because of the dipole−dipole base−base interactions.

Using the new results, we can rule out significant carrier ligand NH to G O6 hydrogen bonding in only the ΔHT1 conformer of **Bip**Pt(dinucleotide) adducts. Our work shows that a G residue with an upfield H8 signal (∼8 ppm) does not necessarily have a canted base with G O6 hydrogen bonding. Thus, hydrogen bonding need not be invoked to explain any results at pH ∼7.5 and below for **Bip**Pt(dinucleotide) HH conformers, suggesting that the hydrogen bonding is weak at best. Rather downfield H8 shifts (ranging from 8.88 to 9.09 ppm) were reported for all H8 signals of the two HH forms of the d(GpG) Pt complex with the **hpip** (homopiperazine) carrier ligand.[72] The authors concluded that the G bases in **hpip**Pt HH adducts have little canting and do not form **hpip** NH to G O6 hydrogen bonds. The H8 shifts reported are similar to those found here for the HH form of the **Me$_2$ppz**Pt(dinucleotide) adducts, which cannot have hydrogen bonds. Thus, our **Me$_2$ppz** results support the conclusions in the **hpip** study.

(72) Hambley, T. W.; Ling, E. C. H.; Messerle, B. A. *Inorg. Chem.* **1996**, *35*, 4663−4668.

Conclusions

Two HH forms (HH1 and HH2) and one HT form were observed as major **Me$_2$ppz**Pt(d(GpG)) conformers, thus marking the first characterization of three major conformers for one *cis*-PtA_2(d(GpG)) adduct. We attribute this finding to the unique minimal steric demand of the tertiary sp^3 nitrogens of the **Me$_2$ppz** carrier ligand. The results are consistent with our previous studies with retro models, showing that chiral carrier ligands with secondary amine donors influence G base canting and thus the relative stability of conformers. The structure of the sugar phosphate backbone changes from conformer to conformer but does not depend on the **Me$_2$ppz** vs the **Bip** carrier ligand. Thus, within the range of base canting observed for these retro models, base canting does not significantly influence the backbone structure.

Comparison of the results *for the ΔHT1 conformer* for **Bip**Pt(dinucleotide) and **Me$_2$ppz**Pt(dinucleotide) adducts establishes that carrier ligand NH to G O6 hydrogen bonding has no influence on base canting and is not a significant stabilizing interaction. The MMD models of the ΔHT1 form of (*S*,*R*,*R*,*S*)-**Bip**Pt(d(GpG)) have distances of 2.94 and 2.07 Å for G O6 to N and to NH, respectively.[34] If the G bases are more canted, even shorter distances are possible. These values are smaller than some values determined for simple models in the solid state,[30−32] for which sufficient water is not present to compete for the NH group. Thus, experimental evidence such as that presented here was needed to establish the weakness of G O6−NH hydrogen bonds in water. Our results are consistent with solid-state data showing that quasi-axial NH groups have weak hydrogen bonds;[48,49] in the solid state, G O6−NH hydrogen bonding is found for quasi-equatorial NH groups exclusively, and the **Bip** ligand has only quasi-axial NH groups. Direct experimental evidence in water for assessing the relative strength of G O6 hydrogen bonds to axial vs equatorial NH's is lacking, however. We believe the weakness of the hydrogen bonding can be seen to be reasonable by considering an important but often neglected aspect of adduct formation: Pt withdraws electron density from the coordinated G base. (The inductive effect is clearly reflected experimentally in the characteristically lower pK_a of the **G** N1H group for **G** ligands bound to Pt than for **G** ligands in solution.[19]) As a consequence, the G O6 has a weakened hydrogen-bond-acceptor ability.

Neither G base in the HH forms of the **Me$_2$ppz**Pt(dinucleotide) adducts is canted; a conformer with uncanted G bases is rare. The results demonstrate that neither G base canting nor G O6 hydrogen bonding is an intrinsic feature of the HH forms. The lack of change in the backbone of the conformers with change in carrier ligand suggests that relatively little energy is needed to change the base canting. The typically observed upfield shift of one of the G H8 signals in HH forms of almost all other small models indicates that the base of that G residue is canted.[21] However, any hydrogen bonding by the G O6 of this residue to the carrier ligand NH is most probably weak and adventitious.

The minimal significance of carrier ligand−G O6 hydrogen bonds indicated by our results for *cis*-PtA_2(dinucleotide)-type adducts brings into question the proposed role of NH groups in accounting for the anticancer activity of *cis*-PtA_2X_2-type compounds. The important feature of an NH group may be its small size, not its hydrogen-bonding ability.

Unless a carrier ligand such as (*R*,*S*,*S*,*R*)-**Bip** (which favors right-handed canting) is present,[24,47] all single-stranded N7−Pt−N7 cross-linked d(GpG) species regardless of oligonucleotide length are left-handed. On duplex formation, the handedness is generally agreed to change to right-handed.[24] However, the recent structural studies[28,29] of both protein-bound and free duplexes with the cross link indicate that the canting of neither base in the cross-link bp step is as large as in small models.[11,73] The structures exhibit very large distortions away from B-form DNA,[28,29] and the distorted duplex structure does not permit strong hydrogen bonding. There is almost no canting of either base in the cross link; however, the bias is right-handed.

We believe the structure of the cross link is influenced by the recently discovered unusual Lippard bp step.[28] Any analysis of duplexes requires that one consider the effect of this bp step. The Lippard bp step has, among other features, unusually large positive slide and shift. This is caused by movement of the 5′-G* bp, whereas the other bp in the step (in the 5′ direction from the lesion) remains more or less in the position expected for B-DNA. As a consequence, if the 5′-G* retained its normal left-handed canting and G O6 hydrogen bonding, the six-membered ring of the 5′-G* base would clash with the adjacent 5′-residue. These steric clashes will easily overcome the forces favoring H-bonding and canting of the 5′-G*, which this work shows are weak. As we have suggested previously,[29] the distorted features in duplexes should be considered in drug design. For example, the carrier ligand should not strongly favor a particular canting direction because the distortions found in the duplexes may no longer be possible.

Acknowledgment. This work was supported by NIH Grant GM 29222 (to L.G.M.). We thank Prof. Giovanni Natile (University of Bari) for helpful discussions and MURST, the University of Bari, and the University of Lecce for financial support. We thank the reviewers for helpful comments.

Supporting Information Available: Descriptions of ^{1}H NMR signal assignments for **Me$_2$ppz**Pt(GpG) and **Me$_2$ppz**Pt(d(GpG)); table of **Me$_2$ppz**Pt(d(GpG)) and **Me$_2$ppz**Pt(GpG) conformer distribution as a function of pH; H8 region of **Me$_2$ppz**Pt(GpG) NOESY spectrum; **Me$_2$ppz**Pt(GpG) ^{1}H−^{31}P HMBC spectrum; H8 region of **Me$_2$ppz**Pt(d(GpG)) NOESY spectrum; 1D NOE experiment with **Me$_2$ppz**Pt(d(GpG)) showing an NOE between the H8 signals of the less dominant HH conformer (HH2); **Me$_2$ppz**Pt(d(GpG)) ^{1}H−^{31}P HMBC spectrum; discussion of HH1 and HH2 conformer assignment for **Me$_2$ppz**Pt(d(GpG)); and regions of the **Me$_2$ppz**Pt(d(GpG)) ROESY spectrum showing H8−H8 NOE and NOEs between H8 signals and sugar resonances (PDF). This material is available free of charge via the Internet at http://pubs.acs.org.

JA010483M

(73) Admiraal, G.; van der Veer, J. L.; de Graaff, R. A. G.; den Hartog, J. H. J.; Reedijk, J. *J. Am. Chem. Soc.* **1987**, *109*, 592−594.